PROTON BAND CROSSING IN THE SUPERDEFORMED NUCLEUS ^{144}Gd*

R.M. LIEDER, ST. UTZELMANN, W. GAST, A. GEORGIEV,

PH. HOERNES,

Institut für Kernphysik, Forschungszentrum Jülich
D-52425 Jülich, Germany

S. LUNARDI, D. BAZZACCO, R. MENEGAZZO, C. ROSSI-ALVAREZ,

Dipartimento di Fisica and Istituto Nazionale di Fisica Nucleare,
Sezione di Padova, I-35131 Padova, Italy

G. DE ANGELIS, D.R. NAPOLI AND M. DE POLI

Istituto Nazionale di Fisica Nucleare
Laboratori Nazionali di Legnaro, Via Romea 4, I-35020 Legnaro, Italy

(Received October 24, 1994)

The features of the superdeformed band in ^{144}Gd have been studied. An $i_{13/2}$ proton crossing has been observed in ^{144}Gd which is absent in the isotope ^{146}Gd. This has been explained as a deformation effect. The absence of this crossing in the superdeformed bands of the neighbouring $N = 80$ isotones of ^{144}Gd can be understood in terms of a blocking effect.

PACS numbers: 21.60.Ev

1. Introduction

The experimental investigations of the $Z = 64$ isotopes $^{144,146-150}$Gd [1–7] and of the $N = 80$ isotones ^{142}Sm [8], ^{143}Eu [9] and ^{145}Tb [10] proved the existence of one or several superdeformed bands in each of these nuclei. These data provided a wealth of nuclear structure information involving

* Presented at the XXIX Zakopane School of Physics, Zakopane, Poland, September 5–14, 1994.

band crossings [1, 2, 4–6], cross-talk between bands [6] and identical bands [5, 11]. These data helped to establish the configurations of the superdeformed bands in these nuclei.

The superdeformed bands have been classified according to the occupation number of high–N intruder orbitals, where N is the main oscillator quantum number [12, 13]. In ^{146}Gd two protons occupy the $N = 6$ $i_{13/2}$ orbital and one neutron is in the $N = 7$ $j_{15/2}$ orbital; in a short notation this is written as $\pi 6^2 \nu 7^1$. All superdeformed bands observed in $^{146-148}$Gd and the yrast superdeformed band in ^{149}Gd are considered to have the same $\pi 6^2 \nu 7^1$ configuration [7]. A band crossing in a superdeformed band has been found for the first time in ^{146}Gd [2]. It is caused by the crossing of $i_{13/2}$ and $i_{11/2}$ neutron orbitals. The crossing frequency is $\hbar\omega = 0.65$ MeV. Similar band crossings have subsequently been also observed in superdeformed bands of $^{147-149}$Gd [4, 5].

From theoretical predictions ^{144}Gd was expected to be a good candidate for the observation of superdeformation [12, 14, 15]. To search for a superdeformed band in this nucleus, several experiments have previously been performed [16–18], but none was successful so that this case remained a challenge for a long time. Only very recently a superdeformed band has been found in ^{144}Gd [1]. In the present paper some features of the superdeformed band in ^{144}Gd will be discussed.

2. Bandcrossing in the superdeformed band of ^{144}Gd

The superdeformed band in ^{144}Gd has been established [1] in an experiment with the γ-spectrometer GASP using the reaction ^{100}Mo + ^{48}Ti at a beam energy of 221 MeV. The beam was provided by the XTU tandem accelerator of the Laboratori Nazionali di Legnaro (LNL). The nucleus ^{144}Gd was produced in this experiment in the $4n$ channel. In order to obtain more information on the superdeformed band in ^{144}Gd recently a second GASP experiment with the same reaction at a beam energy of 215 MeV was carried out at the LNL. The target consisted of three self-supporting foils of ^{100}Mo with a total thickness of 1.1 mg/cm^2. The collected events have been sorted into a three dimensional E_γ-E_γ-E_γ array (cube), unpacking events of fold $F > 3$ into triple events, under the condition that the multiplicity measured with the BGO ball was larger than 8. Furthermore, proper gates were used to select events of large sum energy of the BGO ball and a time window was set in order to include only prompt γ-rays. With these conditions 1.5 Giga triple events were available in the cube for further analysis. A double-gated coincidence spectrum of the superdeformed band in ^{144}Gd is shown in Fig. 1. The spacings between consecutive γ-rays is decreasing from 55 keV at large γ-ray energies to 40 keV at $\approx$900 keV and

three close lying transitions can be seen at ≈890 keV. The assignment of the superdeformed band to ^{144}Gd follows from the observation of strong transitions placed above the 10^+ isomer in ^{144}Gd [19] in coincidence with clean transitions of the superdeformed band.

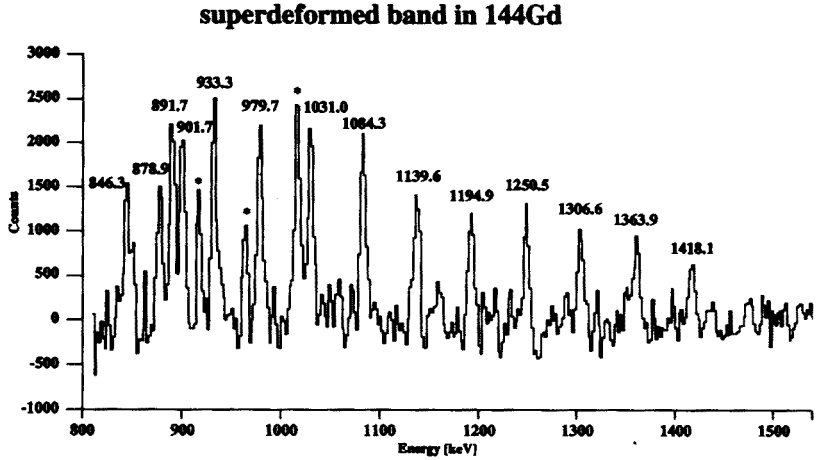

Fig. 1. Sum of double-gated coincidence spectra showing the superdeformed band in ^{144}Gd. Gates have been set on all transitions of the superdeformed band. The band members are marked by their energies and known transitions in ^{144}Gd are denoted by a *.

The three close lying transitions at ≈890 keV (*cf.* Fig. 1) indicate that the superdeformed band in ^{144}Gd undergoes a band crossing at a rotational frequency of $\hbar\omega = 0.45$ MeV. The present data set seems to support the previous ordering of the 902 keV and the 892 keV transitions [1], *viz.* that the 892 keV transition has to be placed above the 902 keV transition in the superdeformed band. The superdeformed band deexcites from the three lowest-lying members just below the band crossing.

The experimental dynamic moment of inertia of the superdeformed band in ^{144}Gd is compared in Fig. 2 with theoretical predictions of Nazarewicz *et al.* [12]. The experimental results show a pronounced band crossing at a rotational frequency of $\hbar\omega = 0.45$ MeV. This band crossing is much more pronounced than those observed in $^{146-148}$Gd. At higher frequencies the dynamic moment of inertia assumes values of ≈72 $\hbar^2$/MeV similar to those observed for the superdeformed bands of the heavier Gd nuclei [11]. For the superdeformed band of ^{144}Gd it is from theoretical calculations [12] predicted that at low frequencies the $\pi i_{13/2}$ orbitals and most probably also the $\nu j_{15/2}$ orbitals [20] are not occupied but that four $\nu i_{13/2}$ orbitals are populated. The superdeformed well arises from large shell gaps for $N = 80$ and $Z = 64$ [12]. When the nucleus is cranked the aligned $\pi 6^2$ configuration

approaches rapidly the Fermi-surface. The observed band crossing in ^{144}Gd is thus interpreted as a crossing of the $\pi 6^0$ configuration with the aligned $\pi 6^2$ configuration. After the crossing the superdeformed band in ^{144}Gd has either a $\pi 6^2 \nu 7^0$ or a $\pi 6^2 \nu 7^1$ configuration. The fact that the band crossing is fairly sharp indicates a small interaction between the two superdeformed structures. The experimental results reproduce rather well the predicted band crossing [12]. This is the first experimental observation of a crossing in a superdeformed band related to the alignment of a proton pair.

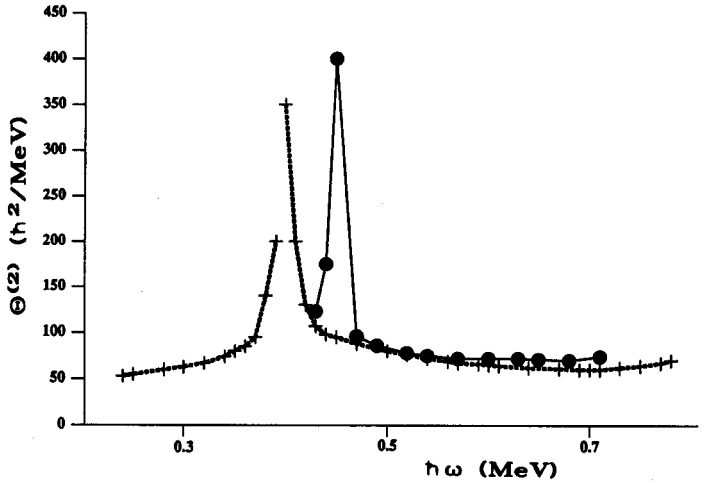

Fig. 2. Comparison of the experimental dynamic moment of inertia of the superdeformed band in ^{144}Gd with theoretical predictions of Nazarewicz *et al.*

Plots of the dynamic moment of inertia as function of rotational frequency for the superdeformed bands in ^{144,146}Gd are shown in Fig. 3. It is interesting to note that the $i_{13/2}$ proton band crossing, seen in ^{144}Gd, does not show up in ^{146}Gd although the configuration is considered to be the same and the proton number has not changed. The only plausible explanation is, that this is a deformation effect. In order to study the deformation dependence of the band crossing behaviour in more detail cranked shell model (CSM) calculations [21] have been carried out. In this model the motion of quasiparticles in a potential rotating with the frequency $\hbar\omega$ is studied. The single-particle states are calculated using the Nilsson potential. The calculations have been performed for deformation parameters of $0.44 < \epsilon_2 < 0.60$ and $\epsilon_4 = 0.02$ and 0.05 considering that Nazarewicz *et al.* [12] calculated $\epsilon_2 = 0.48$ and $\epsilon_4 = 0.02$ for the superdeformed nucleus ^{146}Gd and $\epsilon_2 = 0.44$ and $\epsilon_4 = 0.05$ for the superdeformed nucleus ^{144}Gd at the low angular momentum end of the superdeformed band. In Fig. 4 results of the CSM calculations for quasiproton states of positive parity are shown for the deformation parameters corresponding to ^{146}Gd (upper por-

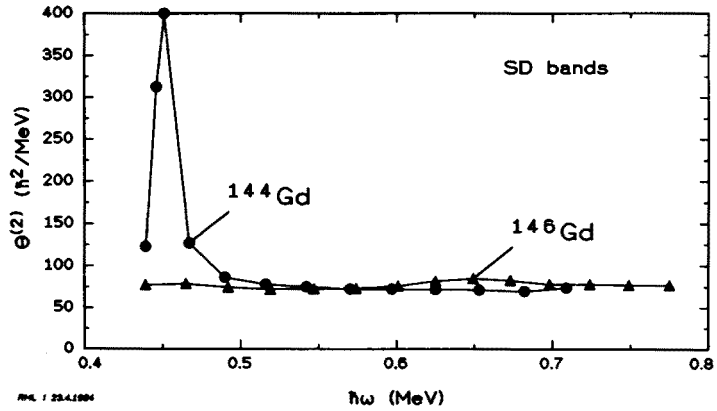

Fig. 3. Experimental dynamic moment of inertia as function of rotational frequency for the yrast superdeformed bands in ^{144,146}Gd.

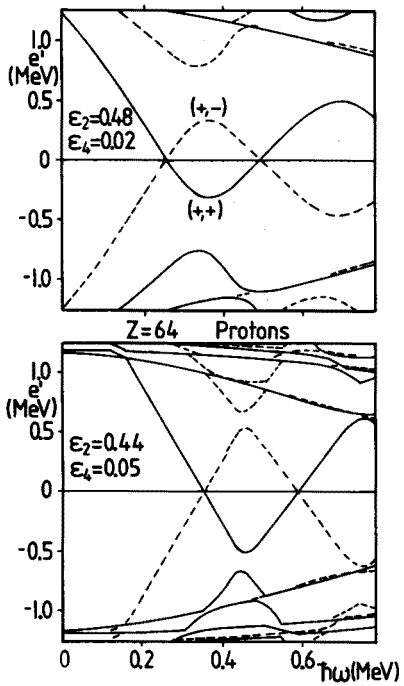

Fig. 4. Routhian diagram for quasiproton states of positive parity for Gd nuclei ($Z = 64$) as obtained in cranked shell model calculations. The deformation parameters ϵ_2 and ϵ_4 are given in the figure. A γ-deformation of $\gamma = 0$ and a pair gap of $\Delta = 1.17$ MeV was used.

tion) and ^{144}Gd (lower portion). It can be seen that the first excited $i_{13/2}$ quasiproton state lowers very rapidly in energy with increasing rotational frequency and that a crossing occurs. Significant differences in the crossing frequencies and interaction strengths can be recognized in the two diagrams representing different deformations.

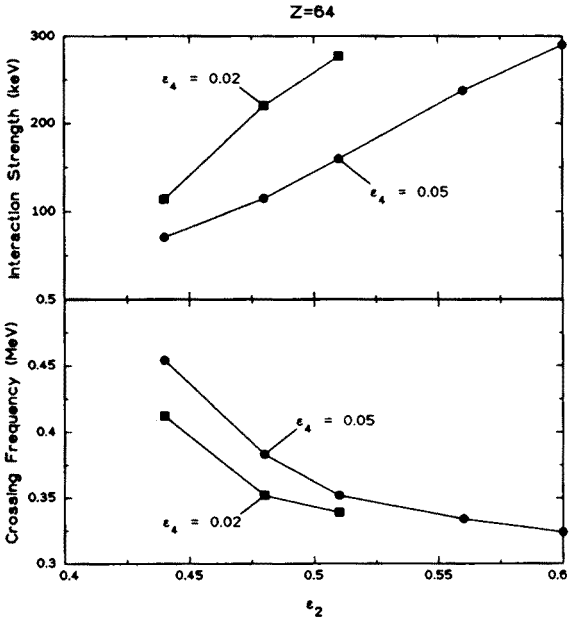

Fig. 5. Crossing frequency and interaction strength as function of the deformation parameter ϵ_2 for Gd nuclei.

The crossing frequency and the interaction strength are plotted as function of ϵ_2 in Fig. 5 for the intersection involving the first excited $i_{13/2}$ quasiproton state. It can be seen that the crossing frequency decreases and the interaction strength increases with increasing deformation ϵ_2. For the deformation parameters of ^{144}Gd ($\epsilon_2 = 0.44$ and $\epsilon_4 = 0.05$) a sharp crossing (small interaction strength) at a frequency of $\hbar\omega = 0.45$ MeV is expected as found experimentally. For the deformation parameters of ^{146}Gd ($\epsilon_2 = 0.48$ and $\epsilon_4 = 0.02$) the $i_{13/2}$ proton crossing is shifted to $\hbar\omega = 0.35$ MeV and the interaction strength is large. In the presently available data for ^{146}Gd [2] this crossing cannot be observed since the superdeformed band starts at a rotational frequency of $\hbar\omega = 0.44$ MeV. The different band crossing behaviour related to the alignment of a pair of $i_{13/2}$ protons in ^{144}Gd and ^{146}Gd can hence be explained satisfactorily as a deformation effect.

3. Systematics of superdeformed bands in the isotones of ^{144}Gd

For the $N = 80$ isotones ^{142}Sm [8], ^{143}Eu [9], ^{144}Gd [1] and ^{145}Tb [10] the dynamic moment of inertia is plotted as function of the rotational frequency in Fig. 6. It can be seen that none of the isotones of ^{144}Gd shows the strong $i_{13/2}$ proton crossing observed in this nucleus. The superdeformed bands in ^{142}Sm, ^{143}Eu and ^{145}Tb exhibit a rather constant moment of inertia. The absence of band crossing could be explained as a blocking effect if at least one $i_{13/2}$ proton orbital is populated in these nuclei. Actually, a $\pi 6^1 \nu 6^4 \nu 7^0$ configuration has been assigned to the superdeformed band in ^{143}Eu [9, 12]. The configuration of the superdeformed band in ^{142}Sm is considered to have the same configuration as that in ^{143}Eu coupled to a hole in the $[541]\frac{1}{2}^-$ Nilsson orbital [8]. For ^{145}Tb a $\pi 6^1 \otimes ([404]\frac{9}{2}^+)^2$ configuration has been suggested [10] for the superdeformed band. Hence, in all three isotones of ^{144}Gd the $i_{13/2}$ proton orbital is blocked so that the absence of band crossing can be understood.

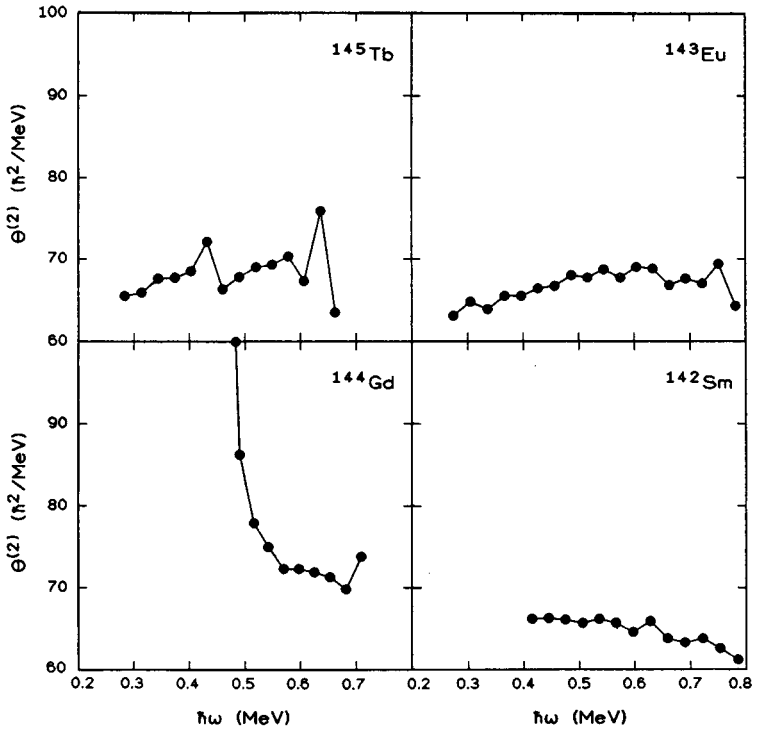

Fig. 6. Plots of the dynamic moment of inertia vs. rotational frequency for superdeformed bands observed in several $N = 80$ isotones.

4. Population of superdeformed bands in the Gd nuclei

An investigation of the intensities of the superdeformed bands in $^{146-149}$Gd has been carried out by Haas *et al.* [7] utilizing Si beams. The results are given in Table I. In this table also the intensities of the superdeformed bands in ^{144}Gd [1], excited in a ^{48}Ti induced reaction, and in ^{146}Gd [2], excited in a ^{40}Ar induced reaction, are included. Although different reactions were used to excite the superdeformed bands in the various Gd nuclei, which may lead to a different population, as will be discussed subsequently, one can conclude that the intensity decreases with mass number.

TABLE I

Intensities of yrast superdeformed bands relative to the total intensities of the produced nuclei.

Nucleus	Reaction	E_{beam} (MeV)	$I_\gamma(SD)/I_\gamma(total)$	Reference
^{149}Gd	^{124}Sn(^{30}Si,5n)	155	3.3±0.3	Haas *et al.*
^{148}Gd	^{124}Sn(^{29}Si,5n)	155	1.30±0.15	Haas *et al.*
^{147}Gd	^{122}Sn(^{30}Si,5n)	155	0.87±0.19	Haas *et al.*
^{146}Gd	^{110}Pd(^{40}Ar,4n)	175	≈1.0	Hebbinghaus *et al.*
^{146}Gd	^{122}Sn(^{29}Si,5n)	155	0.65±0.19	Haas *et al.*
^{145}Gd	^{120}Sn(^{30}Si,5n)	155	<0.4	Haas *et al.*
^{144}Gd	^{100}Mo(^{48}Ti,4n)	221	≈0.2	Lunardi *et al.*

If a certain nucleus is populated by means of different reactions it is possible to relate the intensity of the superdeformed band to the spin distribution of the entry states. In Fig. 7 spin distributions are shown for various reactions which have been used to populate superdeformed bands in ^{144,146}Gd. They are plotted as insets in diagrams of the excitation energy vs. angular momentum which include the normal and superdeformed yrast states. The spin distributions have been calculated with the Julian–Pace code. From the results for ^{146}Gd one can draw conclusions about the experimental conditions to optimally populate superdeformed states. They are fed from entry states with large angular momentum and one can see that the high-spin entry states are populated in the ^{40}Ar induced reaction with a larger partial cross section than in the ^{29}Si induced reaction. Correspondingly, the yrast superdeformed band in ^{146}Gd is in the former reaction more strongly populated than in the latter one (*cf.* Table I).

From the above observations one can conclude that the superdeformed band in ^{144}Gd was previously not observed for two reasons:

1. The superdeformed band in ^{144}Gd is too weakly populated in the ^{28}Si induced reaction to allow for an observation (*cf.* Fig. 7). A stronger population as provided by the ^{48}Ti induced reaction is needed.
2. The sensitivity of the γ-detector array GASP at the LNL was needed to observe such a weak superdeformed band.

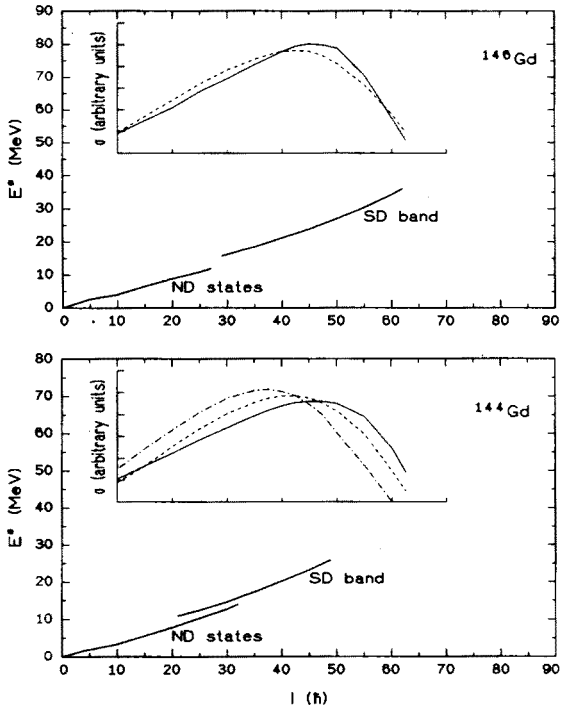

Fig. 7. Excitation energy vs. spin for ^{144,146}Gd. The spin distributions of the entry states relevant for the used reactions and beam energies are plotted as insets. For ^{144}Gd (lower portion) the reactions are denoted as —— ^{100}Mo(^{48}Ti,4n), 215 MeV, - - - ^{100}Mo(^{48}Ti,4n), 221 MeV, — - — - ^{120}Sn(^{28}Si,4n), 145 MeV. For ^{146}Gd (upper portion) the reactions are denoted as —— ^{110}Pd(^{40}Ar,4n), 175 MeV - - - ^{122}Sn(^{29}Si,5n), 155 MeV.

It remains an open question why the superdeformed band in ^{144}Gd has a much smaller intensity than expected theoretically.

We would like to thank the XTU Tandem accelerator staff of the Laboratori Nazionali di Legnaro for providing the beams. The technical assistance of Mr. H.M. Jäger is greatly appreciated.

REFERENCES

[1] S. Lunardi, D. Bazzacco, C. Rossi-Alvarez, P. Pavan, G. de Angelis, D. De Acuna, M. De Poli, G. Maron, J. Rico, O. Stuch, D. Weil, S. Utzelmann, P. Hoernes, W. Satuła, R. Wyss, *Phys. Rev. Lett.* **72**, 1427 (1994).

[2] G. Hebbinghaus, T. Rzaca-Urban, C. Senff, R.M. Lieder, W. Gast, A. Krämer-Flecken, H. Schnare, W. Urban, G. de Angelis, P. Kleinheinz, W. Starzecki, J. Styczen, P. von Brentano, A. Dewald, J. Eberth, W. Lieberz, T. Mylaeus, A. v. d. Werth, H. Wolters, K.O. Zell, S. Heppner, H. Hübel, M. Murzel, H. Grawe, H. Kluge, *Phys. Rev. Lett.* **59**, 2024 (1987); G. Hebbinghaus, K. Strähle, T. Rzaca-Urban, D. Balabanski, W. Gast, R.M. Lieder, H. Schnare, W. Urban, H. Wolters, E. Ott, J. Theuerkauf, K.O. Zell, J. Eberth, P. von Brentano, D. Alber, K.H. Maier, W. Schmitz, E.M. Beck, H. Hübel, T. Bengtsson, I. Ragarsson, S. Åberg, *Phys. Lett.* **B240**, 311 (1990).

[3] T. Rzaca-Urban, K. Strähle, G. Hebbinghaus, D. Balabanski, W. Gast, R.M. Lieder, H. Schnare, W. Urban, P. von Brentano, A. Dewald, J. Eberth, E. Ott, J. Theuerkauf, H. Wolters, K.O. Zell, D. Alber, K.H. Maier, E.M. Beck, H. Hübel, W. Schmitz, *Z. Phys.* **A339**, 421 (1991).

[4] K. Zuber, D. Balouka, F.A. Beck, Th. Byrski, D. Curien, G. de France, G. Duchêne, C. Gehringer, B. Haas, J.C. Merdinger, P. Romain, D. Santos, J. Styczen, J.P. Vivien, J. Dudek, Z. Szymanski, T.R. Werner, *Phys. Lett.* **B254**, 308 (1991).

[5] S. Flibotte, G. Hackman, Ch. Theisen, H.R. Andrews, G.C. Ball, C.W. Beausang, F.A. Beck, G. Belier, M.A. Bentley, Th. Byrski, D. Curien, G. de France, D. Disdier, G. Duchêne, P. Fallon, B. Haas, V.P. Janzen, P.M. Jones, B. Kharraja, J.A. Kuehner, J.C. Lisle, J.C. Merdinger, S.M. Mullins, E.S. Paul, D. Prévost, D.C. Radford, V. Rauch, J.F. Smith, J. Styczen, P.J. Twin, J.P. Vivien, J.C. Waddington, D. Ward, K. Zuber, *Phys. Rev. Lett.* **71**, 688 (1993).

[6] C.W. Beausang, P. Fallon, S. Clarke, F.A. Beck, Th. Byrski, D. Curien, P.J. Dagnall, G. de France, G. Duchêne, P.D. Forsyth, B. Haas, M.J. Joyce, A.O. Macchiavelli, E.S. Paul, J.F. Sharpey-Schafer, J. Simpson, P.J. Twin, J.P. Vivien, *Phys. Rev. Lett.* **71**, 1800 (1993).

[7] B. Haas, V.P. Janzen, D. Ward, H.R. Andrews, D.C. Radford, D. Prévost, J.A. Kuehner, A. Omar, J.C. Waddington, T.E. Drake, A. Galindo-Uribarri, G. Zwartz, S. Flibotte, P. Taras, I. Ragnarsson, *Nucl. Phys.* **A561**, 251 (1993).

[8] G. Hackman, S.M. Mullins, J.A. Kuehner, D. Prévost, J.C. Waddington, A. Galindo-Uribarri, V.P. Janzen, D.C. Radford, N. Schmeing, D. Ward, *Phys. Rev.* **C47**, R433 (1993).

[9] A. Ataç, M. Piiparinen, B. Herskind, J. Nyberg, G. Sletten, G. de Angelis, S. Forbes, N. Gjørup, G. Hagemann, F. Ingebretsen, H. Jensen, D. Jerrestam, H. Kusakari, R.M. Lieder, G.V. Marti, S. Mullins, D. Santonocito, H. Schnare, K. Strähle, M. Sugawara, P.O. Tjøm, A. Virtanen, R. Wadsworth, *Phys. Rev. Lett.* **70**, 1069 (1993).

[10] S.M. Mullins *et al.*, in Proc. Conf. on Physics from Large γ-Ray Detector Arrays, CONF-940888 (Berkeley), vol. I, p. 11 (1994); S.M. Mullins, N.C. Schmeing, S. Flibotte, G. Hackman, J.L. Rodriguez, J.C. Waddington, L. Yao, H.R. Andrews, A. Galindo-Uribarri, V.P. Janzen, D.C. Radford, D. Ward, J. DeGraaf, T.E. Drake, S. Pilotte, E.S. Paul, to be published in *Phys. Rev.* **C**, (1994).

[11] R.M. Lieder, T. Rzaca-Urban, K. Strähle, G. Hebbinghaus, D. Balabanski, W. Gast, H. Schnare, W. Urban, P. von Brentano, A. Dewald, J. Eberth, E. Ott, J. Theuerkauf, H. Wolters, K.O. Zell, D. Alber, K.H. Maier, E.M. Beck, H. Hübel, W. Schmitz, *Prog. Part. Nucl. Phys.* **28**, 225 (1992).

[12] W. Nazarewicz, R. Wyss, A. Johnson, *Nucl. Phys.* **A503**, 285 (1989).

[13] T. Bengtsson, S. Åberg, I. Ragnarsson, *Phys. Lett.* **B208**, 39 (1988).

[14] R.R. Chasman, *Phys. Lett.* **B187**, 219 (1987).

[15] J. Dudek, W. Nazarewicz, Z. Szymanski, G.A. Leander, *Phys. Rev. Lett.* **59**, 1405 (1987).

[16] J.P. Vivien, A. Nourreddine, F.A. Beck, T. Byrski, C. Gehringer, B. Haas, J.C. Merdinger, D.C. Radford, Y. Schutz, J. Dudek, W. Nazarewicz, *Phys. Rev.* **C33**, 2007 (1986).

[17] Y. Schutz, C. Baktash, I.Y. Lee, M.L. Halbert, D.C. Hensley, N.R. Johnson, M. Oshima, R. Ribas, J.C. Lisle, L. Adler, K. Honkanen, D.G. Sarantites, A.J. Larabee, J.X. Saladin, *Phys. Rev.* **C35**, 348 (1987).

[18] J. Gascon, F. Beck, T. Byrski, G. Duchesnes, B. Haas, J.C. Merdinger, A. Nourreddine, P. Taras, J.P. Vivien, *Z. Phys.* **A329**, 139 (1988).

[19] T. Rzaca-Urban, S. Utzelmann, K. Strähle, R.M. Lieder, W. Gast, A. Georgiev, D. Kutchin, G. Marti, K. Spohr, W. Urban, P. von Brentano, J. Eberth, A. Dewald, J. Theuerkauf, I. Wiedenhöfer, K.O. Zell, B. Bochev, K.H. Maier, H. Grawe, J. Heese, H. Kluge, R. Wyss, *Nucl. Phys.*, in print.

[20] R. Wyss, private communication (1994).

[21] R. Bengtsson, S. Frauendorf, *Nucl. Phys.* **A327**, 139 (1979).